Processing and rheological properties of wheat flour dough and bread containing high levels of soluble dietary fibres blends

S Arufe, Hubert Chiron, Joel Dore, Isabelle Savary-Auzeloux, Luc Saulnier, G Della Valle

Food Research International 97 (2017) 123–132

Contents lists available at ScienceDirect

Food Research International

journal homepage: www.elsevier.com/locate/foodres

Processing & rheological properties of wheat flour dough and bread containing high levels of soluble dietary fibres blends

S. Arufe [a], H. Chiron [b], J. Doré [c], I. Savary-Auzeloux [d], L. Saulnier [b], G. Della Valle [b,*]

[a] Departamento de Enxeñaría Quimica, Universidade de Santiago de Compostela, 15782 Santiago de Compostela, Spain
[b] INRA, UR 1268 Biopolymères Interactions Assemblages (BIA), 44 316 Nantes, France
[c] INRA, UMR 1319 Microbiologie de l'Alimentation au Service de la Santé Humaine (MICALIS), 78352 Jouy-en-Josas, France
[d] INRA, UMR 1019, Unité de Nutrition Humaine (UNH), CRNH Auvergne, 63000 Clermont-Ferrand, France

ARTICLE INFO

Article history:
Received 13 December 2016
Received in revised form 10 March 2017
Accepted 19 March 2017
Available online 24 March 2017

Keywords:
Density
Elongational viscosity
Fermentation
Inulin
Maltodextrin
Pectin
Texture

ABSTRACT

Wheat flour doughs were processed with soluble dietary fibres (DF) added up to 40% (w/w flour). DF were made of a ternary mixture of maltodextrins (MT, 3/5), pectins (PE, 1/5) and inulin (IN, 1/5). The addition of DF decreased the specific mechanical energy developed by the mixer, mainly because of water addition. It increased the ratio of storage moduli and the elongational viscosity of the dough, but decreased the strain hardening index. Energy input and rheological changes at mixing largely explained the decreases of porosity characteristic time and stability time during fermentation. It was possible to add up to 30% DF with a moderate increase of bread density, and 20%, with little change of crumb cellular structure. Hence, the changes of bread crumb texture were not mainly due to bread density, but rather likely to the changes of properties of the intrinsic material. Results obtained by addition of single fibre source, especially inulin, deviated from the main trends observed for texture and rheological properties. These results provide a good basis to design breads with increased dietary fibre content.

1. Introduction

For a healthy diet, a large daily dose of dietary fibre (≥25 g/day) is recommended, that is far higher than the consumption observed in most countries (Anderson et al., 2009). Dietary fibres may be classified according to their solubility, which have significant impact on their physiological functionality (Arcila, Weier, & Rose, 2015). Soluble fibres cover a wide range of ingredients, from oligosaccharides to hydrocolloids, and are known to present prebiotic effects (Angioloni & Collar, 2008; Rosell, Santos, & Collar, 2009). These prebiotic effects may lie in the capacity of these fibres (fructoligosaccharides, arabinoxylanes, or resistant starches for instance) to generate active metabolites such as butyrate and propionate, which are short chain fatty acids produced by degradation of the fibres by the colon microbiota (de Vadder et al., 2014). Many studies on physiological impact of dietary fibres have focused on the effect of a single source of fibres which impacts bacteria consortia (Delzenne, Neyrinck, & Cani, 2013), but seldom address the effect of DF blends, which could favor the bacterial diversity via the production of a wider variety of metabolites signals, butyrate and propionate in particular.

Cereals products provide opportunities to develop foods that deliver health benefits for a large population (Ishwarya & Prabhasankar, 2014). Therefore, bread is a good target for fibre enrichment, which requires substitution of wheat flour in the dough recipe. Besides, the physiological effects of fibre addition in bread have already been studied (see for instance Christensen et al., 2013). However, the accurate interpretation of the results of such studies is not straightforward since the addition of fibres, soluble or insoluble, modifies its structure and texture, especially density, which, in turn, will affect the kinetics of digestion and the availability of nutrients (Saulnier, Micard, & Della Valle, 2014). In addition, these modifications will also affect the rheological properties of dough and its processing until final bread texture, which may be detrimental to its sensory properties (Poutanen, Sozer, & Della Valle, 2014). Therefore, when processing functional foods, like breads enriched in fibres, it is essential to strive to maintain the same texture properties, a point which is often discarded. The use of enzymatic and fermentation or physical (extrusion) processes that can tune the solubility of fibres before incorporation to bread recipes (Arcila et al., 2015; Gomez, Jimenez, Ruiz, & Oliete, 2011; Salmenkallio-Marttila, Katina, & Autio, 2001) may be useful in this purpose. However, there is a need to ascertain the effects of soluble fibres at different stages of breadmaking (mixing, fermenting, baking), with emphasis on dough rheological properties and bread specific volume and texture.

* Corresponding author.
E-mail address: guy.della-valle@inra.fr (G. Della Valle).

http://dx.doi.org/10.1016/j.foodres.2017.03.040
0963-9969/

Indeed, addition of soluble fibres may lead to negative effects on dough properties (Morris & Morris, 2012) regarding water absorption, dough development, elasticity and stickiness, which all affect bread sensory properties, especially by increasing density. The main mechanisms of action of soluble fibres (SF) on dough rheological properties have been described by Courtin and Delcour (2002) in the case of water extractable arabinoxylans, with emphasis on dough behavior during processing. Due to variable hydration properties, SF addition first requires an adjustment of water addition during mixing (Hager et al., 2011; Morris & Morris, 2012). Regarding dough rheological properties, the measurements of linear viscoelastic properties (small amplitude oscillations, SAO) have shown that the increase of storage modulus with SF addition, mainly pentosans, could be attributed to a reinforcement of gluten network (Santos, Monteiro, & Lopes da Silva, 2005; Wang, Hamer, van Vliet, & Oudgenoeg, 2002), although opposite result, network weakening, has been found when adding pentosan (Migliori & Gabriele, 2010) or pectin (Angioloni & Collar, 2008). Results from large strain rheological measurements, out of the linear viscoelastic domain, can be linked to process behavior. However, such works about the effect of SF addition are quite seldom, either because dough containing SF are difficult to handle, due to increased stickiness and modified or because such measurements are less popular than SAO measurements. Using uniaxial compression test, Cavella, Romano, Giancone, and Masi (2008) showed that dough elongational viscosity and strain hardening index decreased when adding up to 9% inulin, which suggest worse gas retention performance during dough fermentation and, consequently, lower final bread volume.

Specific volume (or density) is the main target property of bread and it has been shown to increase with addition of low SF amounts. Generally, crumb texture changes (firmness, hardness), observed when adding arabinoxylans, inulin, extruded bran, β-glucans, can be explained, at first, by density changes (Courtin & Delcour, 2002; Cavella et al., 2008; Peressini & Sensidoni, 2009; Gomez et al., 2011; Hager et al., 2011; Morris & Morris, 2012; Rubel, Pérez, Manrique, & Genovese, 2015). Finally, the effects of SF incorporation on dough and bread properties depend on the type of fibre, the addition level and the step of breadmaking process studied. Actually, the effect of SF addition, at levels larger than 10% of flour substitution, has never been studied at different steps of the breadmaking process, likely because of negative effects on dough properties. Moreover, as opposite effects are sometimes encountered, according to the source of fibres, it may be possible to balance those, i.e. reducing the negative ones, by using a blend of different sources. As mentioned earlier, this could enhance the prebiotic effect by favoring the bacterial diversity.

In this context, our aim was to determine to which extent a blend of soluble fibres could be added to wheat flour dough for breadmaking. In this purpose, inulin, pectin and maltodextrins were added at various levels to wheat flour, either single, or binary and ternary blends and the resulting changes of dough properties and bread texture were assessed with rheological and imaging methods.

2. Materials and methods

2.1. Raw materials and dough compositions

French wheat flour (WF, 13%, g protein/g dry flour, dry basis, d.b., 0.55% ash) was supplied by Moulin Girardeau (France). 3 different soluble dietary fibres (DF) were tested: (1) high methoxyl pectin (PE, Unipectine QC 100, Cargill, Germany), (2) short chain inulin (IN, Instant, DP ≤ 10, Cargill, France) and (3) maltodextrins from tapioca starch, named resistant starch (MT, C ActiStar 11,700, Cargill, France, about 50% crystalline with melting DSC peak at 110 °C), which all dissolved in water, at bare eye. Fresh yeast (Springer Lesaffre, France), dried refined fine salt (Salinor, France) and tap water were used in the bread making experiments.

13 different formulations of wheat flour and DF were studied (Table 1). The control formulation consisted of 2000 g wheat flour, 1240 g tap water, 40 g fresh yeast, 36 g salt and 0.04 g ascorbic acid. Six formulations were obtained by adding a mixture of DF, composed of 60% MT, 20% IN, 20% PE (% g fibre/g total fibre content), at different levels (on flour basis, f.b.): 5%, 10%, 20%, 25%, 30% and 40% (dough # 5, 6, 10, 11, 12, 13, respectively). This DF mixture composition is selected because it aims to optimize microbiota diversity and fermentation processes in the gut for the consumer's health benefit (Endo, Niioka, Kobayashi, Tanaka, & Watanabe, 2013). Then 3 formulations resulted from the individual addition of 4% PE, 4% IN, 12% MT, on flour weight basis (#2, 3, 7), or combined in pairs (#4, 8, 9); both addition levels correspond to the same amount of the fibre ingredient as in formulation containing 20% DF (#10).

Tap water addition was adjusted by an expert baker for each formulation at the end of pre-mixing stage in view of dough behavior and mechanical power measurements, in agreement with the French bread making procedure (AFNOR standard V03-716). This procedure includes a protocol for the breadmaking process and provides an evaluation grid of the dough quality according to six criteria: smoothing aspect, stickiness, consistency, extensibility and slackening. The capacity of the expert baker to reason efficiently over a variety of production contexts about the relations between the flour constituents, the ingredients and the mixing process conditions with the dough quality, defined according to these criteria, has been validated by Kansou, Chiron, Della Valle, Ndiaye, and Roussel (2014).

2.2. Breadmaking procedure

Mixing was carried out in a spiral mixer (Diosna SP12, GmbH, Germany). Mixing protocol consisted of 3 different steps. First, wheat

Table 1
Composition of dough formulations (/2000 g wheat flour basis, f.b.), in maltodextrins from tapioca starch (MT), Inulin (IN) and Pectin (PE), DF the amount of added fibres, (% flour sub.)[a] fibres substituting flour, and MC the water content on total wet basis.

Formulation & symbol	MT (g)	IN (g)	PE (g)	DF (% f. b.)	Fibre (% flour sub.)[a]	Water (% f. b.)	MC (%tot. w.b.)
1 △	0	0	0	0	0.0	64.0	46.5
2 ○	0	0	80	4	3.8	88.0	52.1
3 ●	0	80	0	4	3.8	62.0	44.8
4 □	0	80	80	8	7.4	78.0	48.5
5 ▲	60	20	20	5	4.8	69.3	46.8
6 ▲	120	40	40	10	9.1	78.0	48
7 ●	240	0	0	12	10.7	73.3	46.2
8 ■	240	0	80	16	13.8	87.6	49.0
9 ■	240	80	0	16	13.8	71.7	44.7
10 ▲	240	80	80	20	16.7	93.0	49.4
11 ▲	300	100	100	25	20.0	99.0	49.6
12 ▲	360	120	120	30	23.1	106.0	50.0
13 ▲	480	160	160	40	28.6	122.5	51.3

[a] This value is the mass of DF over the mass of DF + flour.

flour and fibres were mixed at 80 rpm for 6 min in order to homogenize the dry mixture. Secondly, yeast, ascorbic acid and water was added and a pre-mixing step was carried out at 80 rpm during 4 min. Thirdly, a texturing step was performed for 7 min at 160 rpm. Salt was added 5 min before the end of mixing step. The mechanical power supplied to the dough and the temperature of the dough were recorded. Mixing conditions were assessed according to the final temperature increase from the initial value during texturing (ΔT, °C), and to the specific mechanical energy (SME, kJ/kg) computed from the mechanical power, as detailed by Shehzad et al. (2012). Experiments were carried out at least in triplicate.

After mixing, dough fermentation was performed in a proofing cabinet (Panem, France) for 20 min at 27 °C and under 75% relative humidity (RH). Then, dough was separated into 350 g pieces. These pieces were manually rounded, then mechanically moulded (Tregor, France) and finally proofed in individual metallic pans, for 100 min at 27 °C and 75% RH. Finally, dough pieces were scarified, and then baked in a deck oven (Bongard, France) for 25 min at 245 °C (hearth and vault temperatures). 300 mL of steam were added before and after loading. Before characterization, breads were cooled at room temperature for 2 h.

2.3. Dough characterization

2.3.1. Thermomechanical properties

Thermomechanical properties of doughs (without yeast) were measured in a dynamic mechanical analyser (DMA, MK IV, Rheometric Scientific, USA) with a plate-plate geometry (17 mm diameter, 3.2 mm gap). After mixing, dough rested 20 min at ambient temperature (≈25 °C). Then a sample of 0.90 ± 0.05 g was placed between the plates and sealed with paraffin (Super Lube, Bohemia, USA). Experiments were carried out at 1 Hz, in the compression mode at 0.1% of strain. As checked in former studies (Rouille, Chiron, Colonna, Della Valle, & Lourdin, 2010; Shehzad et al., 2012), this value is in the linear viscoelastic domain, and it is assumed that any deviation from this domain during heating can be discarded, or at least supposed to be the same for all dough tested. After loading, samples were rested for 5 min prior to testing, and a constant static force ($=10^{-2}$ N) was applied, of negligible contribution on modulus value, to maintain contact between plates and sample during temperature sweep. Temperature was increased from 25 to 120 °C with a constant heating rate of 3 °C/min by air heated oven. It has been previously checked that at this rate, dough sample temperature remained close to controlled oven temperature (Rouille et al., 2010). Values of viscoelastic moduli (E', E" and tanδ = E"/E') where calculated using RSI Orchestrator software (Rheometric Scientific, USA). Taking into account the similar shape of DMA curves, dough behavior was assessed by the ratio (E'_{max}/E'_{min}), the maximum value of storage modulus (E'_{max}) obtained at ≈72 ± 3 °C, to the minimum value (E'_{min}) obtained at ≈48 ± 3 °C. In spite of some changes of these temperature transitions, likely due to different moisture and SF contents, the analysis of the results was focused on E'_{max}/E'_{min}). Indeed, this ratio reflected the swelling of starch granules and the aggregation of gluten proteins, i.e. network cross-linking. All thermomechanical essays were performed at least in duplicate.

2.3.2. Elongational properties

Rheological measurements were carried out at large bi-elongational strain by Lubricated Squeezing Flow test (LSF) using a traction/compression machine (Instron, Type #1122, USA) with a plate-plate geometry (20 mm diameter, 15 mm gap) equipped with a force sensor (0; 100 N). At the end of mixing, dough samples without yeast (≈5 g) were placed in Teflon cylinders (14 mm height, 20 mm diameter) lubricated with paraffin oil and kept at room temperature for 30 min. Then the homogeneous samples were removed from the cylinders and placed between the plates lubricated with paraffin oil. The cylindrical samples were compressed by the upper plate, attached with a movable crosshead, until a final height of 1 mm, at a constant speed ($v = 5$, 10 and 100 mm/min). The force applied to samples was recorded as function of displacement. Data were processed according to the procedure described by van Vliet (2008). Stress σ, defined as the ratio of measured force F to plates area was plotted against biaxial deformation ε_b:

$$\varepsilon_b = -1/2 \ \ln\left(h(t)/h_0\right) \tag{1}$$

For given deformations ε_b [0.1, 0.25, 0.5, 0.75, 1.0, 1.25], biaxial deformation rate $\dot{\varepsilon}_b$ was calculated:

$$\dot{\varepsilon}_b = -\frac{v}{2h(t)} \tag{2}$$

Then stress σ was plotted against biaxial deformation rate. The average slope of those curves defined n, the flow behavior index. From the same plot, different values of Ln(σ) as function of ε_b may be derived for a given value of $\dot{\varepsilon}_b$. The slope of the curve of ln(σ) versus ε_b, $\left(\frac{\partial \ln\sigma}{\partial \varepsilon_b}\right)_{\dot{\varepsilon}_b=cst}$ defines the strain hardening index SHI. Bi-extensional, or elongational, viscosity η_E, was calculated for each deformation ε_b, plotted against biaxial deformation rate $\dot{\varepsilon}_b$ and fitted by the power law equation (Eq. (3)):

$$\eta_E = \sigma/\dot{\varepsilon}_b = K \cdot \left(\dot{\varepsilon}_b\right)^{n-1} \varepsilon_b{}^{SHI} \tag{3}$$

where K (Pa.s^n) is the consistency index, n the flow behavior index (dimensionless), $n < 1$ reflecting a strain rate-thinning behavior of the dough. All doughs were tested at least twice by LSF.

2.4. Dough fermentation follow-up

Images of a rounded dough piece (m = 25 g) during proofing in a controlled ambience (T = 27 °C, RH = 75%) were acquired every 5 min through digital camera for 240 min, according to the procedure described in detail by Shehzad et al. (2010). Porosity P(t), was computed from dough volume V, assuming a cylindrical symmetry. The dough shape ratio was defined by $S(t) = H/L_{max}$, H and L_{max} being, respectively, the height and the maximum width of the dough sample at a given time. The porosity kinetics can be modeled using a Gompertz function, as first proposed by Romano, Toraldo, Cavella, and Masi (2007):

$$P(t) = a.\ \exp\left(-\ \exp\left(-\frac{b \times e}{a}(t-c)\right)\right) + d \tag{4}$$

where coefficient a is an approximation of the final porosity increase, b is the maximum volume expansion growth rate, i.e., the slope at inflection point, c is the time for inflection point, and d, varying like initial porosity, is such as (a + d) = P(t = +∞) with d ≪ a, and e is the Neper number (≈2.72). During proofing, the dough slowly spreads and exhibits a continuous decrease of the shape ratio S(t), reflecting a loss of stability. When $t < 90$ min, these kinetics can be fitted by an exponential decay:

$$S(t) = (a'-c').\exp^{-t/b'} + c' \tag{5}$$

where a' and c' being the stability at $t = 0$ and $t \to +\infty$, respectively, (a'-c') is the overall loss of dough stability, and b' is the starting time of the stationary phase, i.e. spreading ceases when $t \gg b'$. To avoid any bias due to hand rounding of the dough prior to measurement, all curves were shifted to the same value of initial shape ratio, a' = 0.6. Experiments were carried out at least in duplicate.

2.5. Bread characterization

Bread density, ρ^* (g/cm^3), was calculated from ratio mass/volume. After 2 h of cooling, bread volume was measured by rapeseeds displacement in a volumeter (Chopin Technologies, France). Bread mass was measured using a balance (Mettler, PC 44000, Switzerland). Final moisture content of bread was measured after 24 h applying the French standard NF V 03-707 for cereals and bread, by weighing precisely the weight loss of about 20cm^3 of bread, after 1h30min at 130 °C, under atmospheric pressure.

To define crumb cellular structure, images of bread slices are acquired at a macroscopic scale and analyzed by a grey level granulometric method from mathematical morphology (Lassoued, Babin, Della Valle, Devaux, & Réguerre, 2007). For each bread slice, this procedure leads to granulometric curves that are finally analyzed by Principal Component Analysis (PCA), in order to map the crumb images. For each formulation, ten vertical and central slices (11 mm-thickness) are selected and 3 replicates are achieved after removing the crust area (thickness ≈ 2 mm) from the image.

The amount of crust was determined according to the image analysis procedure described in detail by Della Valle, Chiron, Jury, Raitière, and Réguerre (2012). From this analysis, the total and crust section area, St and Sc were determined, and the crust index derived Ic = Sc/St. The whole experiment was triplicated and mean values of the results were presented.

Finally, bread crumb texture was assessed by means of compression assays. About 16 h after cooling, bread slices, after crust removing, were submitted to a compression using a plate-plate geometry (40 mm of diameter) set on a universal testing machine (Instron #1122, Instron Corporation, Canton, MA, USA). The maximum height (h_0) of slices was measured and the crosshead was moved down at a speed of 50 mm/min and stopped after a distance equal to 2/3 h_0. After compression, the bread was relaxed for 180 s. From the force-displacement signal, the apparent modulus of the crumb, E^*(kPa), was derived from the initial slope. The critical stress σ_c (kPa) and the residual stress σ_r (kPa) were obtained, respectively, at the first shoulder, i.e. at the end of the first linear part, of the stress curve, and at the end of the relaxation step.

2.6. Statistical analysis

The goodness of fitting of experimental data to the different models applied was evaluated from the corresponding coefficients of determination (R^2) and root mean square error (E_{RMS}). Differences among means were identified by one-factor analysis of variance (ANOVA), followed by the Scheffe test and considering significant *P*-values ≤ 0.05 (IBM SPSS Statistics 22). In addition, from the repetitions of the experiments, standard deviations were computed and error bars were included in the graphs presenting results.

3. Results and discussion

3.1. Water addition and mixing

As shown in Table 1, the level of water added was generally increased when soluble fibre blend was added. Same trend is observed when adding β-glucan (Hager et al., 2011). However, when inulin was added alone (dough #3), the level of water was decreased, because the dough softened or stuck to the bowl. Similar effect has already been observed by Peressini and Sensidoni (2009) and Hager et al. (2011), especially for short chain inulin. It was attributed to the lubricating effect of inulin oligosaccharides, as we first suggested for sugars and wheat grain oligosaccharides (Rouille, Della Valle, Lefebvre, Sliwinski, & vanVliet, 2005). As a consequence of water addition, the specific mechanical energy, SME, applied to the dough during mixing varied from 24.8 kJ/kg (#5) to 13.5 kJ/kg (#2) (Table 2). This trend, shown in Fig. 1a, did not include the dough with inulin (#3) nor that with inulin and maltodextrin (#9). For these two doughs, lower values of SME might be attributed to the lubricant action of inulin. Conversely, when compared to the amount of DF added, the value of SME reached for dough containing pectin alone (#2) was low (Fig. 1b), likely because of the large amount of water added. All over, the formulations made from the ternary blend of DF led to a regular decrease of SME with the amounts of water and DF added. Similar result has been reported by Le Bleis, Chaunier, Chiron, Della Valle, and Saulnier (2015), who observed a decrease in the same range of SME values (30-15 kJ/kg) when adding insoluble fibres (wheat bran particles). However, in our case, we believe that this decrease should be attributed to the lubricant action of water more than to a deficient development of the gluten network. Indeed, in the latter case, the mechanisms of dough transport in the bowl during mixing would have been changed as a consequence of increased heterogeneity, which has not been observed in our case. Finally, a linear correlation is found between SME and the final dough temperature T_d, for all doughs (not shown, values in Table 2, $R^2 > 0.9$). This result confirmed that heat was transferred to the dough by viscous dissipation of the mechanical energy.

3.2. Rheological properties

As expected, the variations of the storage modulus E' with temperature exhibited first a smooth decrease at a temperature close to 50 °C, where it took a minimum value E'_{min}, followed by a strong increase until T ≈ 75 °C, where it took a maximum value E'_{max} (Fig. 2a). The values of E'_{max}/E'_{min}, are assumed to reflect the thermal sensitivity and

Table 2
Mixing characteristics and rheological properties of dough formulations (/2000 g wheat flour basis, f.b.). Figures in bold indicate minimum and maximum values. Standard deviations were <4% for mixing energy and temperature, and <12% for values derived from rheological measurements.

Formulation & symbol	Fibre (% f.b.)	SME (kJ/kg)	T_d (°C)	K (kPa s^n)	n	SHI (Pa)	E'_{max}/E'_{min}
1 △	0	24.4	23.1	7.6	0.29	2.05	14.5
2 ○	4	**13.5**	**20.1**	6.8	**0.22**	1.98	11.7
3 ●	4	23.4	23.0	10.2	**0.40**	2.07	**18.2**
4 □	8	17.9	21.2	13.6	0.30	1.88	8.0
5 ▲	5	**24.8**	**23.3**	6.4	0.25	2.18	15.9
6 ▲	10	19.0	21.4	6.1	0.26	**2.25**	13.0
7 ●	12	20.3	22.2	6.9	0.27	1.75	15.0
8 ■	16	20.1	21.3	13.7	0.30	1.79	10.6
9 ■	16	17.9	21.7	**5.2**	**0.22**	2.05	13.8
10 ▲	20	16.3	20.6	11.3	0.34	1.80	12.1
11 ▲	25	16.1	20.5	10.4	0.28	1.65	10.0
12 ▲	30	15.3	20.3	10.1	0.27	1.58	7.5
13 ▲	40	15.0	**20.1**	**17.5**	0.36	**1.25**	**5.5**

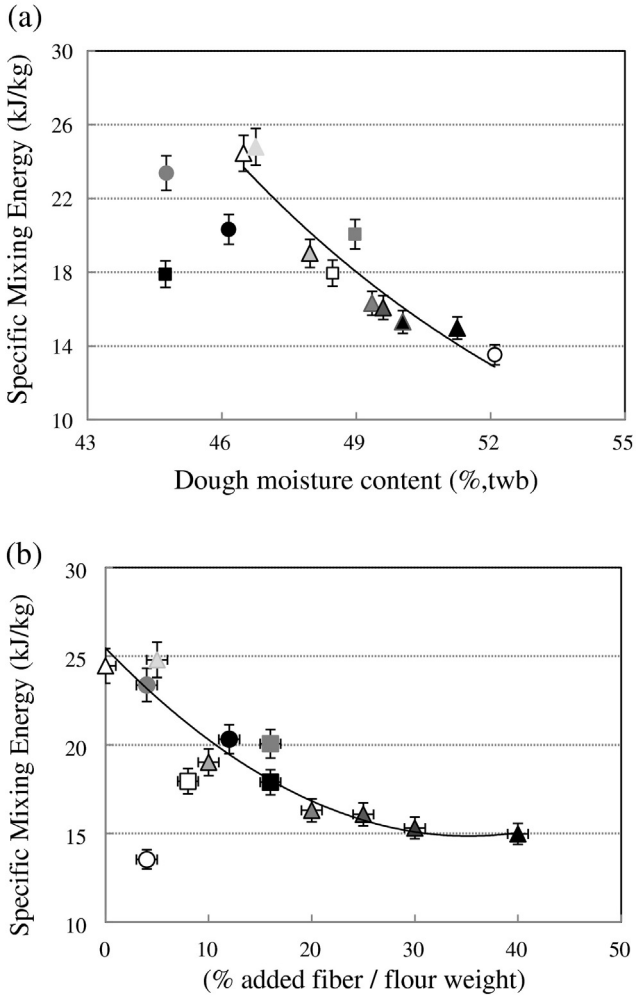

Fig. 1. Variations of specific mechanical energy during dough mixing with (a) water content and (b) with the amount of fibres added for the formulations described in Table 1. Correlations ($r^2 = 0.93$ and 0.94, respectively) are drawn for control dough (△) and doughs containing ternary blend of fibres (▲, 5; ▲, 10; ▲, 20; ▲, 25; ▲, 30; ▲, 40% on flour basis). Binary blends are indicated by □ (PE/IN), ■ (PE/MT) and ■ (IN/MT) and single ingredient formulation are indicated by ○ (PE), ● (IN), ● (MT).

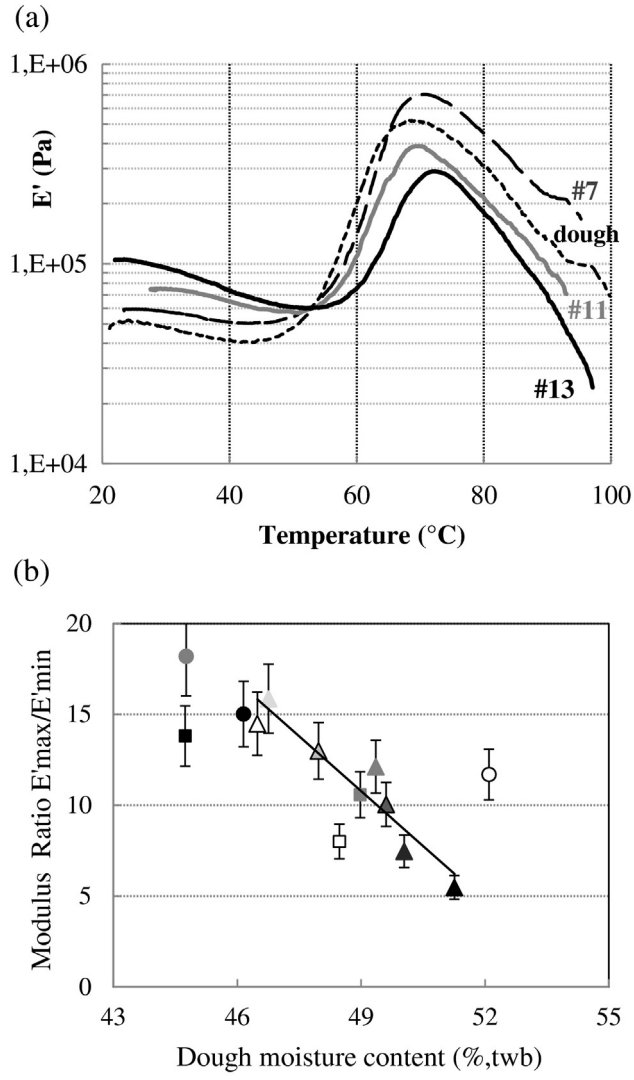

Fig. 2. Dynamic Thermomechanical Analysis (DMA) of doughs: (a) typical variations of storage modulus E' with temperature for control dough (#1, ——), with SF addition 12% MT (#7, — —), 25% (#11, ——), and 40% ternary blend (#13, —); (b) moduli ratio E'_{max}/E'_{min}, with dough moisture content. Correlation curves ($r^2 = 0.9$) is drawn only for control dough and doughs containing ternary blend of fibres (triangle symbols, same legend as indicated for Fig.1, and also in Tables 1 & 2).

the behavior of the dough. They decreased from 18.2 for the dough containing only inulin (#3) to 5.5, for the dough containing the largest amount of DF (#13) (Table 2). These variations are marked by an overall decrease of thermal sensitivity when large amounts of DF added (Fig. 2b). Since the value of E'_{max} rather remained constant, this trend is thought to be due to the increase of E'_{min} value, because of the thickening of the liquid phase. It is in agreement with the commonly observed trends, either for soluble pentosans from wheat (Santos et al., 2005), or long chains inulin (Cavella et al., 2008). Nevertheless, it should be recalled that a decrease of modulus has been found by Hager et al. (2011) and Rubel et al., (2015) when adding inulin. Likely the size of the oligosaccharides chains used may explain this apparent contradiction. Supramolecular organization (crystallinity) may also be inferred for the effect of added maltodextins as suggested for type IV resistant starches by Haralampu (2000).

The biaxial extension measurements performed at different strain values ($0.1 < \dot{\varepsilon}_b < 1.25$) for the 13 dough formulations, confirmed that the variations of elongational viscosity (η_E) could be adjusted by the power law, function of strain rate $\dot{\varepsilon}_b$ indicated in Eq. (3), as illustrated by flow curve segments presented in Fig. 3a. For strain values $\varepsilon_b =$ 0.75, the values.

of consistency index (K) varied between 5.2 kPa·s^n (#9) and 17.5 kPa.s^n (#13) whereas the flow index values (n) varied in a narrow interval (0.22 to 0.4) and the strain hardening index values (SHI), derived for $\dot{\varepsilon}_b = 10^{-2}\ s^{-1}$, varied between 1.25 and 2.25 (Table 2). These values were in the interval of values reported in the literature for various processing conditions and compositions (Launay & Michon, 2008; Turbin-Orger, Shehzad, Chaunier, Chiron, & Della Valle, 2016; van Vliet, 2008). The values of K were generally lower than those found by Le Bleis et al. (2015) for dough enriched with insolube fibres (wheat bran). A concomitant increase of K and decrease of SHI was observed when moisture content, and the amount of ternary blend added, increased (Fig. 3 b, c). This trend was also observed for other fibres except when adding pectins alone (#2, O). Clearly, these opposite trends cannot be interpreted by the action of a charge in a suspension, unlike for (solid) bran particles in dough (Le Bleis et al., 2015). To our knowledge, these results have never been observed before, except SHI decrease already found for the addition of long chain inulin (Cavella et al., 2008) and also qualitatively by Wang et al. (2002) in the case of water extractable pentosans (WEP). At first glance, it could be attributed to dilution effects of the gluten network by increased water amount. However

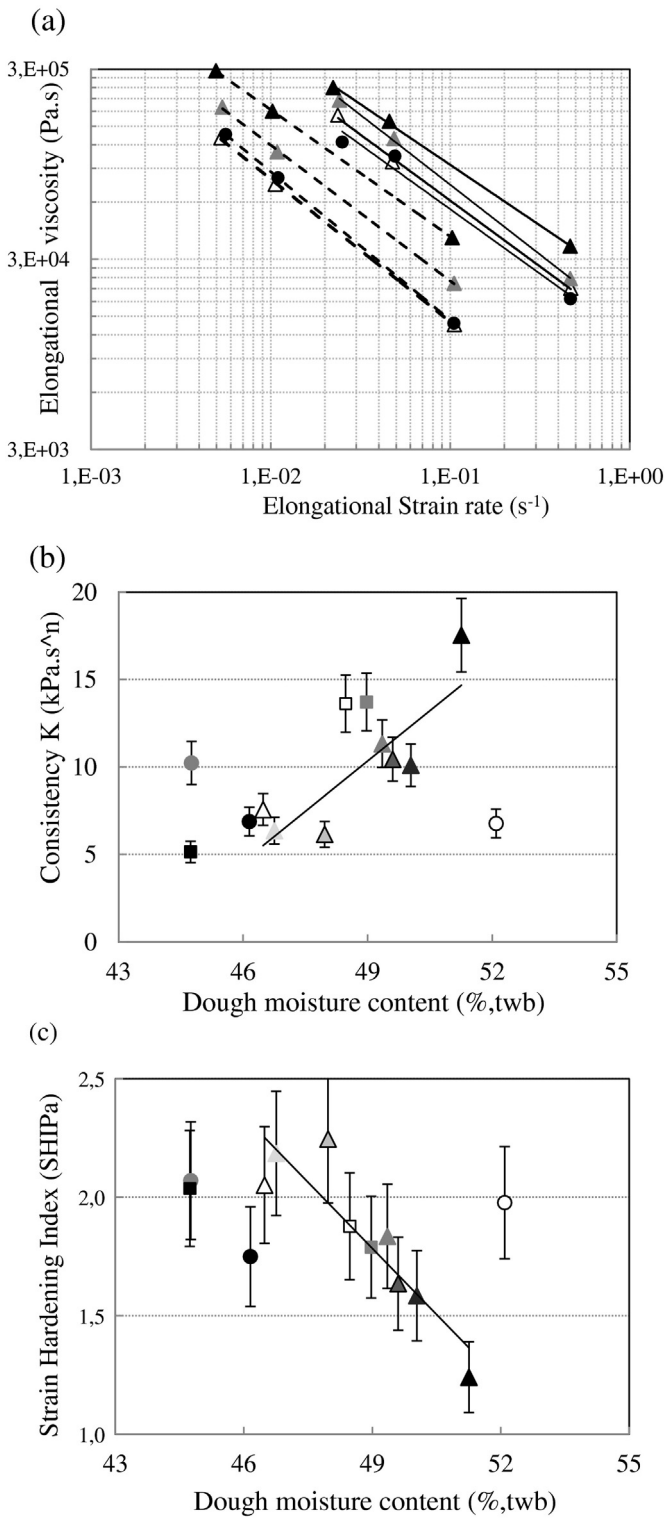

Fig. 3. Elongational properties of doughs measured by LSF: (a) typical variations of elongational viscosity with strain rate at constant strain values $\varepsilon_b = 0.25$(dotted lines) and $\varepsilon_b = 1$ (cont. line) for control dough (#1, △), with SF addition 12% MT (#7, ●), 25% (#11, ▲), and 40% ternary blend (#13, ▲); variations with dough moisture content of (b) consistency index K and (c) strain-hardening index SHI. Correlation curves ($r^2 =$ 0.76 and 0.82, respectively) are drawn only for control dough and doughs containing ternary blend of fibres (triangle symbols, same legend as indicated for Fig. 1, and also in Tables 1 & 2).

the increase of consistency (Fig. 3b) rather suggests that a thickening of the liquid phase by soluble fibres might counteract the dilution by water.

3.3. Dough behavior during proofing

The kinetics of porosity and stability of dough during fermentation were determined at macroscopic scale by 2D image follow-up. The porosity curves had a sigmoid shape with a final value (a + d at $t =$ 240 min) between 0.7 and 0.8 (see insert in Fig. 4a). These curves were well fitted by the Gompertz model (Eq. (2), $R^2 > 0.99$), for all dough formulations. The relative standard deviation of porosity parameters (a, b, c, d) was <8%. Given this uncertainty, the porosity increase (a) remained constant $= 0.72 \pm 0.04$ except for dough #13 (a = 0.63) which has the largest DF (Table 3). A decrease of dough expansion during fermentation has also been found for larger levels (7 to 10% of flour substitution) of long chain inulin addition (Cavella et al., 2008; Peressini & Sensidoni, 2009). The time for inflection point (coefficient c), or porosity characteristic time, varied between 30 ± 1 min for the dough containing only maltodextrins (#7) and an average value of 49 ± 3 min for doughs containing high amounts of ternary blend (#11, 12). These values were lower than those found by Le Bleis et al. (2015) for dough enriched with wheat bran, likely because of the larger viscosity of

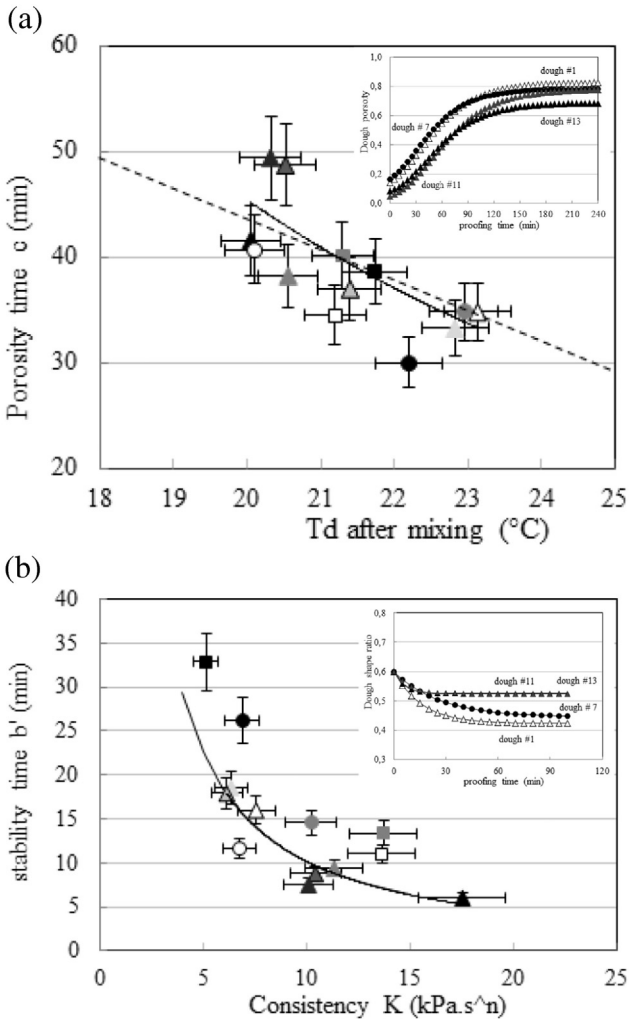

Fig. 4. Dough behavior during fermentation: (a) variations of porosity characteristic time c with dough temperature at the end of mixing Td, with inserted examples of porosity kinetics for dough #1 (control, △), #7 (12% MT, ●), #11 (25% fibres, ▲) and #13 (40% fibres, ▲), dotted line standing for the results from Turbin-Orger et al. (2016) and (b) variations of stability characteristic time b' with dough consistency K with inserted examples of stability kinetics for dough #1 (control, △), #7 (12% MT, ●), #11 (25% fibres, ▲) and #13 (40% fibres, ▲). Correlation curves ($r^2 = 0.62$ (a), 0.89 (b)) are drawn for control dough and doughs containing ternary blend of fibres (triangle symbols, same legend as indicated for Fig. 1, see also in Tables 1 & 2).

Table 3
Characteristic coefficients of dough fermentation kinetics defined by Eqs. (2) & (3). Figures in bold indicate minimum and maximum values. Standard deviations were <8% for porosity coefficients and <10% for stability coefficients.

Formulation & symbol	Fibre (% f.b.)	Porosity				Stability	
		a	b (10^3 min^{-1})	c (min)	d	b' (min)	c'
1 △	0	0.73	7.7	35	0.1	16	**0.42**
2 ○	4	**0.76**	7.1	41	0.07	12	0.46
3 ●	4	0.745	**11.5**	35	**0**	15	**0.42**
4 □	8	0.73	6.1	34	**0.13**	11	0.49
5	5	0.74	6.7	33	0.12	19	0.47
6 ▲	10	0.73	**6.3**	37	0.12	18	0.44
7 ●	12	0.67	7.6	**30**	0.11	26	0.445
8 ■	16	0.74	6.7	40	0.07	13	0.51
9 ■	16	0.71	9.5	39	0.03	**33**	0.43
10 ▲	20	**0.76**	8	38	0.03	9	**0.53**
11 ▲	25	**0.76**	7.2	**49**	0.03	9	0.52
12 ▲	30	0.73	7.1	**49**	0.02	7	0.54
13 ▲	40	**0.63**	6.5	42	0.06	**6**	0.525

Dough & bread with soluble fibres Arufe et al.

these latter doughs, as indicated by K values. However they were larger than those found by Turbin-Orger et al. (2016) who managed to obtain large variations of SME and, consequently, of dough temperature at the end of mixing. Although T_d varied in a much narrower interval in our case (3 °C), we found a similar decreasing trend for the variations of porosity characteristic time with T_d (Fig. 4a). This trend was explained by the yeast activation and gas production, due to larger dough temperature at the start of fermentation. To avoid this influence of dough temperature on the porosity increase of dough with SF addition, it would be necessary to process dough in a mixing system with temperature control in order to obtain variations of dough final temperature <3 °C. In line, the scattering of the data might be due to two main mechanisms: (1) larger amount of maltodextrins (#7), partly containing sugars, might have increased gas production and speeded up dough expansion, hence leading to lower c values, in line with the findings of Romano et al. (2007) on the influence of yeast activity on porosity kinetics, (2) dough containing larger amounts of ternary blend (especially #11, 12), having larger viscosity, displayed larger values of c: a high elongational viscosity decreases the growth of gas bubbles, hence slowing down dough expansion.

Dough spreading during proofing was reflected by the continuous decrease of the shape ratio S(t), which was well fitted by an exponential decay (Eq. (3), $R^2 > 0.9$), for $t \leq 90$ min (see insert in Fig. 4b). The relative standard deviation of stability coefficients (b', c') was <10%. The asymptotic value, or final stability, c', varied in a narrow range, from 0.42 to 0.53, compared with the values found earlier by addition of fat and sucrose, adding bran or modifying mixing conditions, (Le Bleis et al., 2015; Shehzad et al., 2010; Turbin-Orger et al., 2016). This comparison shows that dough containing soluble fibres did not spread much. Conversely, the starting time of the stationary phase (b') varied between 6 min (#13) and 33 min (#9) (Table 3), which suggests that these doughs rapidly ceased to spread, or stabilized. Extensive spreading or loss of stability is clearly undesirable and is often associated with internal collapse due to gas cell coalescence, as found by Turbin-Orger et al. (2015), who showed that fermented dough could be envisioned as a three phases medium, in which gas bubbles are finally separated by liquid films. Hence, the negative correlation of the characteristic time of stability with elongational viscosity reflects the resistance of dough to bubble coalescence, improving dough stability (Fig. 4b). Clearly, at longer fermentation times (t > c > b'), the dough cellular structure could be stabilized by liquid films, the viscosity of which would be increased by the presence of polysaccharides contained in soluble fibres. This is particularly illustrated by the lower values of b' obtained for dough containing pectins (#2, 4, 8).

3.4. Bread texture

3.4.1. Density, crust and cellular structure of breads

DF did not change so much the density of bread crumb, the values of which remained in the interval 0.21–0.25 $g \cdot cm^{-3}$, except for bread containing only maltodextrins and inulin (#9; 0.3 $g \cdot cm^{-3}$) and bread with largest DF (#13, 0.39 $g \cdot cm^{-3}$) (Table 4). These results are in agreement with Peressini and Sensidoni (2009) who reported an increase of density up to 0.33 $g \cdot cm^{-3}$, with addition of larger amounts of long chain inulin (>7% of flour substitution). The density of the crumb was linearly correlated to the one of bread ($R^2 = 0.82$, graph not shown) and the lack of fit might be attributed to the differences observed on crust, as discussed in the following. The moisture content of the crumb varied between 45% and 51% (wb) and was highly correlated to the one of the dough ($R^2 = 0.95$, not shown).

The crust index derived from the ratio of surface areas, determined by image analysis of bread slice, varied from 0.004 (# 13) to 0.086 ± 0.01 (#3). This maximum value corresponds to an average crust thickness of 2 mm. For ternary blends, crust index tends to decrease with pan bread density (Fig. 5a). Indeed crust is formed during baking when the external layer of dough reaches low moisture content, and its temperature increases beyond 100 °C. So, this general decreasing trend may be explained by the larger moisture content of the breads having a larger DF content (see also Fig.1a). Moreover, the larger density of these doughs could decrease the internal heat transfer, and then slow down the formation of crust during baking (Della Valle et al., 2012). Conversely, the larger I_c values of doughs containing inulin and maltodextrins (# 3, 7, 9) do not follow this general trend. This result might be related to lower moisture content and more intense browning reactions due to short chain glucans.

The cellular structure was mainly governed by the density. For example, crumb #1 had a rather uniform and smooth grain (Fig. 6a). By contrast, sample #13, with largest DF, gave a smaller bread volume, in agreement with large density value, and it had a coarser and more heterogeneous cell structure, as shown by larger cells and thicker walls. In comparison, other samples, with intermediate DF, exhibited little variations in cell sizes and cell wall thickness, in line with density values close to the one of control bread (#1). Granulometric curves obtained from bread images were submitted to principal component analysis (PCA) and bread crumbs were compared on a similarity map (Fig. 6b). The first principal component, accounting for 92% of total granulometry variance, mainly underlined the regular increase of differences in average cell size and cell wall thickness for breads with increasing DF content, but without marked increase of cellular heterogeneity, except for #13, thus confirming images observation. This result is somewhat different from the one obtained with the addition of insoluble fibres (bran

Table 4
Texture properties of pan breads enriched with soluble fibres. Figures in bold indicate minimum and maximum values. Standard deviations were <7% for density values, 25% for crust index and 15% for mechanical properties.*

Formulation & symbol	Fibre (% f. b.)	Density, moisture and crust				Mechanical properties		
		bread ($g \cdot cm^{-3}$)	crumb ($g \cdot cm^{-3}$)	MC (tb, %)	I_c (−)	E* (kPa)	σ_c (kPa)	σ_r (kPa)
1 △	0	$0.215^{a,b}$	**0.210^{a}**	$46.0^{a,b,c}$	$0.054^{b,c,d,e}$	$5.80^{a,b}$	$0.50^{a,b}$	2.00^{a}
2 ○	4	**$0.205^{a,b}$**	$0.235^{a,b,c}$	50.9^{e}	$0.022^{a,b}$	$5.25^{a,b}$	**$0.40^{a,b}$**	1.60^{a}
3 ●	4	$0.240^{b,c,d}$	0.260^{c}	**44.5^{a}**	**0.086^{e}**	22.55^{c}	1.45^{e}	4.40^{c}
4 □	8	0.215^{a}	**0.210^{a}**	$48.6^{c,d,e}$	$0.028^{a,b,c}$	$7.15^{a,b}$	$0.45^{a,b}$	**1.40^{a}**
5 ▵	5	0.213^{a}	$0.240^{a,b,c}$	$46.3^{a,b,c}$	$0.022^{a,b}$	11.50^{b}	$0.85^{c,d}$	3.25^{b}
6 ▲	10	$0.223^{a,b}$	$0.240^{a,b,c}$	$47.9^{b,c,d}$	$0.017^{a,b}$	11.35^{b}	$0.80^{c,d}$	2.95^{b}
7 ●	12	$0.235^{a,b,c}$	$0.240^{a,b,c}$	$45.3^{a,b}$	$0.064^{c,d,e}$	$8.70^{a,b}$	$0.70^{b,c}$	$3.55^{b,c}$
8 ■	16	$0.235^{a,b}$	$0.225^{a,b}$	$49.8^{d,e}$	$0.036^{a,b,c,d}$	$7.65^{a,b}$	$0.55^{a,b,c}$	1.95^{a}
9 ■	16	$0.291^{c,d}$	0.300^{d}	$45.1^{a,b}$	$0.074^{d,e}$	**27.20^{c}**	**1.85^{f}**	**7.65^{d}**
10 ▲	20	$0.238^{a,b}$	$0.220^{a,b}$	$49.7^{d,e}$	$0.019^{a,b}$	$7.10^{a,b}$	$0.45^{a,b}$	1.75^{a}
11 ▲	25	$0.258^{a,b,c}$	$0.225^{a,b}$	$50.0^{d,e}$	$0.023^{a,b,c}$	**4.75^{a}**	**0.40^{a}**	1.45^{a}
12 ▲	30	0.292^{d}	$0.250^{b,c}$	$50.3^{d,e}$	0.012^{a}	$6.00^{a,b}$	$0.45^{a,b}$	1.65^{a}
13 ▲	40	**0.398^{e}**	**0.385^{e}**	**$51.4^{d,e}$**	**0.004^{a}**	11.72^{b}	1.00^{d}	$3.90^{b,c}$

*Data are presented as mean values ± standard deviation. Data value of each parameter with different superscript letters in columns are significantly different Scheffe test; $p \leq 0.05$.

particles), that leads to more uniform but much coarser crumbs (Le Bleis et al., 2015). However, in both cases, the change of cellular structure seemed to be only governed by the increase of density.

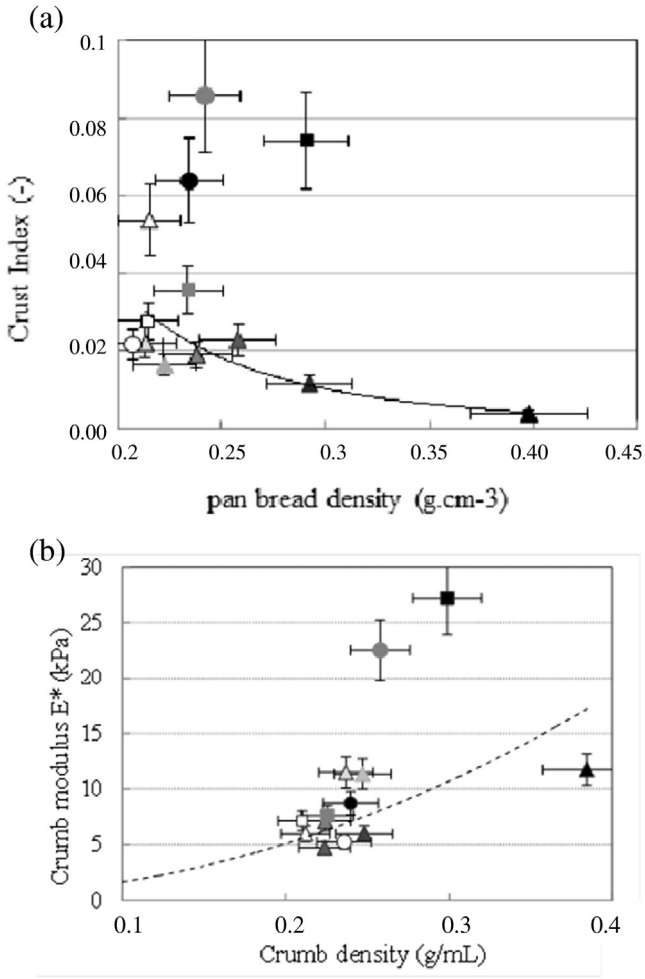

Fig. 5. Bread characteristics: (a) variations of crust index of pan bread with density, correlation curve ($r^2 = 0.79$) is drawn for control dough and doughs containing ternary blend of fibres (triangle symbols), and (b), variations of crumb modulus E* with density ρ^* = dotted line represents the trend indicated by open solid foam model (exponent $n = 2$, Eq. (6)). Same symbols as indicated for Fig. 1 (see also in Tables 1 & 2).

3.4.2. Crumb mechanical properties

Results from compression–relaxation test led to various texture properties as reported in Table 4. The modulus of crumb E*, related to its firmness, varied from 5.25 k Pa for the bread containing PE (#2), to 27.2 k Pa for crumb containing MT and IN (#9) whereas the control bread had a low E* value (5.8 kPa) and the bread containing the larger DF (#13) led to a crumb with intermediate value of modulus E* = 11.7 kPa. The relative standard deviation for these variables was ±12%. Values found for the critical and residual stresses, σ_c and σ_r, varied in the same ratio, and were highly correlated to E* values ($R^2 = 0.84$ and 0.87, respectively). This result indicated that modulus values can well characterize the texture of these crumbs. Values measured for E* were slightly larger than those reported by Guessasma, Chaunier, Della Valle, and Lourdin (2011) (E* = 4–16 kPa) for breads of lower density ($\rho^* \leq 0.2\ g \cdot cm^{-3}$). Crumb modulus tended to increase with density, but this result cannot be predicted by the model of cellular solids: $E^* \sim \rho^{*n}$ (Gibson & Ashby, 1997), as shown by the lack of correlation in Fig. 5b. The theoretical value of n is 2 for open foams, but lower values ($1 \leq n \leq 1.75$) have been found for bread crumbs, by Zghal and Sapirstein (2002). Divergence from the model of cellular solids may be due to differences in (1) cellular structure and (2) the intrinsic properties of the crumb material. Difference in cellular structure is unlikely, since, as discussed before, image analysis did not reveal strong differences in crumb grain (see Fig. 6b). So it might be rather imparted to the crumb material. Indeed, Fig. 5b shows that the discrepancy is largely due to crumbs containing inulin only (#3, ●), and its blend with maltodextrins (# 9, ■). The influence of the cell wall material could be taken into account in the more accurate formulation of the cellular solids model for open solid foam (Gibson & Ashby, 1997):

$$E^*/E_s \approx (\rho^*/\rho_s)^n \quad (6)$$

where E_s is the intrinsic modulus of the crumb material, which depends on its composition and inner structure. Unfortunately, values of E_s are presently unknown, especially for crumb materials containing SF. Indeed, larger E_s value for crumbs containing inulin (#3), and its blend with maltodextrin (#9), would improve the fitting with relation (Eq. (6)). This hypothesis is worth to be worked on because it suggests a reinforcement of the mechanical properties of the wall material. It is in line with the values of consistency, which were found higher than expected for dough containing inulin (Fig. 2b). So it remains a perspective for further investigation on dough at microscopic level.

4. Main findings and conclusions

A ternary blend containing 3/5 tapioca maltodextrins, 1/5 pectins and 1/5 inulin was tested in order to determine to which extent soluble

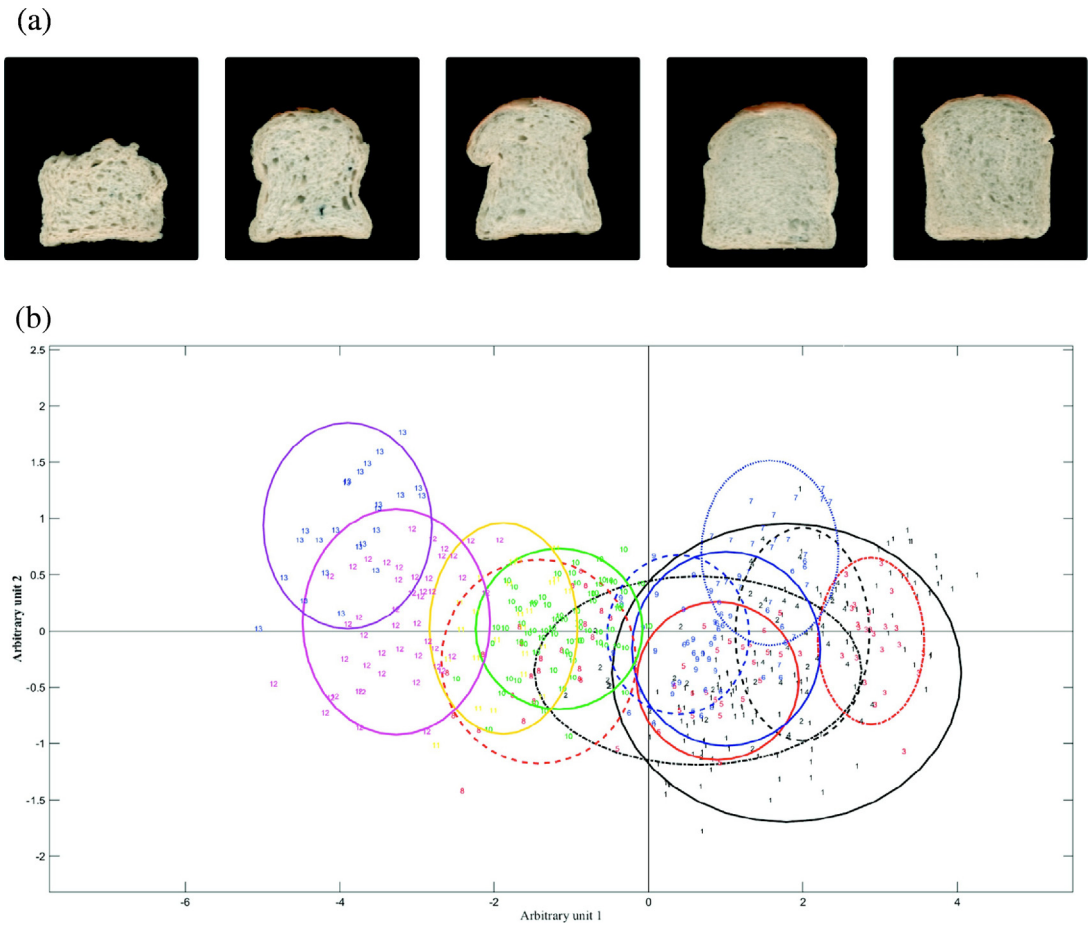

Fig. 6. Cellular structure of bread crumb illustrated by (a) images of bread slices (from right to left: #1, 6, 10, 12, 13) and (b) similarity map of crumb images granulometry after image analysis, each ellipse featuring a set of slices, indicated by a number, come from the same bread; x axis (principal component 1) explains 92% of total granulometry variance.

fibres could be added to wheat flour dough for breadmaking. By adding up to 40% of this blend, with adjusted water addition during mixing, a wide range of dough rheological properties was covered and general trends were observed for dough enriched with the ternary blend. Although the separate addition of single soluble fibre, mainly inulin, led to results which could escape to these general trends, these trends are worth to be recalled here, from both practical and scientific viewpoints.

First, the addition of water, increased with the amount of added soluble fibres, decreased energy requirements during mixing, and hence final dough temperature. We also showed that the main effect of soluble fibre addition was to increase dough elongational viscosity, and to decrease strain hardening index, in relation with the amount of water added. Small deformation studies (DMA) suggest that this increase of dough viscosity could be due to the increase of dough liquid phase viscosity rather than to direct interactions of polysaccharide components with gluten network. Except for largest fibre addition (DF > 30%), a large porosity increase of the dough was obtained during fermentation. This increase was delayed for dough expansion having larger fibre content, likely because of lower final dough temperature after mixing. Conversely, the stability of the dough was improved by adding soluble fibres, for all compositions, whatever the fibre origin, a result which could be imparted to the increased viscosity of liquid films separating gas bubbles. Finally, the texture changes of bread enriched with the soluble fibres were well taken into account by the variations of elastic modulus E*. However, the variations of E* values with density were not in agreement with the open solid foam model. This discrepancy suggested that texture changes were not only governed by the density, but likely involved a change of crumb cell walls properties, mainly in the presence of inulin.

Finally, this work shows that it is possible to process breads having large content of soluble with density and texture closed to those of control bread, provided that the level of added ternary blend of fibres is less or equal to 30%, i.e. 23% of wheat flour substitution, or 15% on overall bread mass. Given the importance of bread density and texture on nutritional properties, this result opens prospects for nutritional studies and, in the longer term, for the design of breads with improved nutritional properties on targeted human populations. In addition, from a practical point of view, the knowledge of the rheological properties will be helpful to assess the main effects of the addition of soluble dietary fibres on dough and bread properties.

Acknowledgements

This study was funded by INRA in the frame of the AGIR project, in which all partners are gratefully acknowledged. Authors are also particularly thankful to Cargill for fibres donation and especially Mrs. Douwina Boscher for useful discussions.

Nomenclature

a, b, c, d	Parameters of the Gompertz model for porosity P
a', b', c'	Parameters of the exponential decay for stability
DF	Amount of soluble dietary fibres added to the wheat flour (% flour)
E^*, E_s	Apparent and intrinsic modulus of bread crumb and cell wall material, respectively (Pa)
	E'_{max}, E'_{min} Maximum and minimum values of dough storage modulus measured by DMA (Pa)
I_c	Crust index of bread, determined by image analysis

IN, MT, PE	Inulin, Maltodextrin, Pectin, soluble fibres added to wheat flour
K, n	Consistency and flow indices of dough elongational viscosity ($Pa \cdot s^n$, -)
MC	Moisture content of dough, crumb, or bread, on a total wet basis (%)
P(t)	Dough porosity (-)
RH	Relative Humidity
S(t)	Dough shape ratio (-)
SHI	Strain Hardening Index of dough (Pa)
SME	Specific mechanical energy at mixing (kJ/kg)
T_d	Dough temperature at the end of mixing (°C)
ΔT	Temperature rise during mixing = (T_t-T_f) (°C)
ε_b, $\dot{\varepsilon}_b$	biaxial elongational strain (-),strain rate (biaxial) (s^{-1})
η_E	Elongational viscosity ($Pa \cdot s$)
ρ^*, ρ_s	Density of crumb and gas-free dough ($g \cdot cm^{-3}$)
σ_c, σ_r	Critical and residual stress for crumb during compression and at the end of relaxation (Pa)

References

Anderson, J. W., Baird, P., Davis, R. H., Ferreri, S., Knudtson, M., Koraym, A., ... Williams, C. L. (2009). Health benefits of dietary fiber. *Nutrition Reviews*, *67*, 188–205.

Angioloni, A., & Collar, C. (2008). Functional response of diluted dough matrixes in high-fibre systems: A viscometric and rheological approach. *Food Research International*, *41*, 803–812.

Arcila, J. A., Weier, S. A., & Rose, D. J. (2015). Changes in dietary fiber fractions and gut microbial fermentation properties of wheat bran after extrusion and bread making. *Food Research International*, *74*, 217–223.

Cavella, S., Romano, A., Giancone, T., & Masi, P. (2008). The influence of dietary fibres on bubble development during bread making. In G. M. Campbell, M. G. Scanlon, & D. L. Pyle (Eds.), *Bubbles in Food 2 - Novelty, Health and Luxury* (pp. 311–322). St Paul, USA: Eagan Press.

Christensen, K. L., Hedemann, M. S., Laerke, H. N., Jorgensen, H., Mutt, S. J., Herzig, K. H., & Bach Knudsen, K. E. (2013). Concentrated arabinoxylan but not concentrated beta-glucan in wheat bread has similar effects on postprandial insulin as whole-grain rye in porto-arterial catheterized pigs. *Journal of Agricultural and Food Chemistry*, *61*, 7760–7768.

Courtin, C. M., & Delcour, J. A. (2002). Arabinoxylans and endoxylanases in wheat flour bread-making. *Journal of Cereal Science*, *35*, 225–243.

Della Valle, G., Chiron, H., Jury, V., Raitière, M., & Réguerre, A. L. (2012). Kinetics of crust formation during conventional French bread baking. *Journal of Cereal Science*, *56*, 440–444.

Delzenne, N. M., Neyrinck, A. M., & Cani, P. D. (2013). Gut microbiota and metabolic disorders: How prebiotic can work? *The British Journal of Nutrition*, *109*, S81–S85.

Endo, H., Niioka, M., Kobayashi, N., Tanaka, M., & Watanabe, T. (2013). Butyrate-producing probiotics reduce nonalcoholic fatty liver disease progression in rats: New insight into the probiotics for the gut-liver axis. *PloS One*, *8*, 63–88.

Gomez, M., Jimenez, S., Ruiz, S., & Oliete, B. (2011). Effect on extruded wheat bran on dough rheology and bread quality. *LWT- Food Science and Technology*, *44*, 2231–2237.

Guessasma, S., Chaunier, L., Della Valle, G., & Lourdin, D. (2011). Mechanical modelling of cereal solid foods. *Trends in Food Science and Technology*, *22*, 142–153.

Hager, A. S., Ryan, L. A. M., Schwab, C., Gänzle, M. G., O'Doherty, J. V., & Arendt, E. K. (2011). Influence of the soluble fibres inulin and oat β-glucan on quality of dough and bread. *European Food Research Technology*, *232*, 405–413.

Haralampu, S. G. (2000). Resistant starch – A review of the physical properties and biological impact of RS. *Carbohydrate Polymers*, *41*, 285–292.

Ishwarya, S. P., & Prabhasankar, P. (2014). Prebiotics: Application in bakery and pasta products. *Critical Review in Food Science & Nutrition*, *54*, 511–522.

Kansou, K., Chiron, H., Della Valle, G., Ndiaye, A., & Roussel, P. (2014). Predicting the quality of wheat flour dough after mixing by modelling expert's know-how. *Food Research International*, *64*, 772–782.

Lassoued, N., Babin, P., Della Valle, G., Devaux, M. F., & Réguerre, A. L. (2007). Granulometry of bread crumb grain: Contributions of 2D and 3D image analysis at different scale. *Food Research International*, *40*, 1087–1097.

Launay, B., & Michon, C. (2008). Biaxial extension of wheat flour dough: Lubricated squeezing flow and stress relaxation properties. *Journal of Texture Studies*, *39*, 496–529.

Le Bleis, F., Chaunier, L., Chiron, H., Della Valle, G., & Saulnier, L. (2015). Processing wheat flour dough and French bread enriched with wheat bran. *Journal of Cereal Science*, *65*(167–174), 2015.

Migliori, M., & Gabriele, D. (2010). Effect of pentosane addition on dough rheological properties. *Food Research International*, *43*, 2315–2320.

Santos, D. M. J., Monteiro, S. R., & Lopes da Silva, J. A. (2005). Small strain viscoelastic behavior of wheat gluten-pentosan mixtures. *European Food Research and Technology*, *221*, 398–405.

Morris, C., & Morris, G. A. (2012). The effect of inulin and fructo-oligosaccharide supplementation on the textural, rheological and sensory properties of bread and their role in weight management: A review. *Food Chemistry*, *133*, 237–248.

Peressini, D., & Sensidoni, A. (2009). Effect of soluble dietary fibre addition on rheological and breadmaking properties of wheat doughs. *Journal of Cereal Science*, *49*, 190–201.

Poutanen, K., Sozer, N., & Della Valle, G. (2014). How can technology help to deliver more of grain in cereal foods for a healthy diet? *Journal of Cereal Science*, *59*, 327–336.

Romano, A., Toraldo, G., Cavella, S., & Masi, P. (2007). Description of leavening of bread dough with mathematical modelling. *Journal of Food Engineering*, *83*, 142–148.

Rosell, C. M., Santos, E., & Collar, C. (2009). Physico-chemical properties of commercial fibres from different sources: A comparative approach. *Food Research International*, *42*, 176–184.

Rouille, J., Chiron, H., Colonna, P., Della Valle, G., & Lourdin, D. (2010). Dough/crumb transition during French bread baking. *Journal of Cereal Science*, *52*, 161–169.

Rouille, J., Della Valle, G., Lefebvre, J., Sliwinski, E., & vanVliet, T. (2005). Shear and extensional properties of bread doughs affected by their minor components. *Journal of Cereal Science*, *42*, 31–43.

Salmenkallio-Marttila, M., Katina, K., & Autio, K. (2001). Effects of bran fermentation on quality and microstructure of high-fiber wheat bread. *Cereal Chemistry*, *78*, 429–435.

Saulnier, L., Micard, V., & Della Valle, G. (2014). Structure du pain et index glycémique. *Cahiers de nutrition et diététique*, *49*(61–66), 2014.

Shehzad, A., Chiron, H., Della Valle, G., Kansou, K., Lamrini, B., & Lourdin, D. (2012). Energetical and rheological approaches of wheat flour during mixing with a spiral mixer. *Journal of Food Engineering*, *110*, 60–70.

Shehzad, A., Chiron, H., Della Valle, G., Kansou, K., Ndiaye, A., & Réguerre, A. L. (2010). Porosity and stability of bread dough during proofing determined by video image analysis for different compositions and mixing conditions. *Food Research International*, *43*, 1995–2005.

Turbin-Orger, A., Babin,P., Boller, E., Chaunier, L., Chiron, H., Della Valle, G., Dendievel, R., Réguerre, AL., Salvo, L. (2015). Growth and setting of gas bubbles in a viscoelastic matrix imaged by X-ray microtomography: The evolution of cellular structure in fermenting wheat flour dough. Soft Matter, 11, 3373–3384.

Turbin-Orger, A., Shehzad, A., Chaunier, L., Chiron, H., & Della Valle, G. (2016). Elongational properties and proofing behaviour of wheat flour dough. *Journal of Food Engineering*, *168*, 129–136.

de Vadder, F., Kovatcheva-Datchary, P., Goncalves, D., Vinera, J., Zitoun, C., Duchampt, A., ... Mithieux, G. (2014). Microbiota-generated metabolites promote metabolic benefits via gut-brain neural circuits. *Cell*, *156*, 84–96.

van Vliet, T. (2008). Strain hardening as an indicator of bread-making performance: A review with discussion. *Journal of Cereal Science*, *48*, 1–9.

Wang, M., Hamer, R. J., van Vliet, T., & Oudgenoeg, G. (2002). Interaction of water extractable pentosans with gluten protein: Effect on dough properties and gluten quality. *Journal of Cereal Science*, *36*, 25–37.

Zghal, M.C., Scanlon, M.G, Sapirstein, H.D. (2002). Cellular structure of bread crumbs and its influence on mechanical properties. Journal of Cereal Science 36, 167–176.